Visual Analysis of Billiard Dynamics Simulation Ensembles

Stefan Boshe-Plois[1], Quynh Quang Ngo[1], Peter Albers[2] and Lars Linsen[1]
[1] *Westfälische Wilhelms-Universität Münster, Germany*
[2] *University of Heidelberg, Germany*

Keywords: Ensemble Visualization, Billiard Dynamics.

Abstract: Mathematical billiards assume a table of a certain shape and dynamical rules for handling collisions. Some trajectories exhibit distinguished patterns. Detecting such trajectories manually for a given billiard is cumbersome, especially, when assuming an ensemble of billiards with different parameter settings. We propose a visual analysis approach for simulation ensembles of billiard dynamics based on phase-space visualizations and multi-dimensional scaling. We apply our methods to the well-studied approach of dynamical billiards for validation and to the novel approach of symplectic billiards for new observations.

1 INTRODUCTION

In the theory of mathematical dynamical systems the main question is to investigate the long-term qualitative behavior of a system in terms of certain qualitative facets. Usually, these facets are phenomena like periodicity and recurring patterns. Further, it can be examined whether a system shows stable or chaotic behavior and how robust it is to perturbations. Mathematical billiards form a category of dynamical systems (Birkhoff, 1927). They arise naturally from physical laws of reflection and show connections to problems like the motion of gas particles in a closed environment. While the ultimate goal is to give answers based on theoretical proofs, it is useful to have well-founded suppositions indicating the direction to head. We present visual analysis methods for simulation ensembles of billiard dynamics to form such suppositions.

Billiards are defined on a table and the dynamics are dependent on the shape of the table (Tabachnikov, 2005). If its boundary is defined via a function, a perturbation corresponds to slightly changing a parameter in the function. The question is what changes occur due to such a perturbation, i.e., whether the billiard trajectories exhibit a qualitatively different behavior. Since it is a priori unclear, which trajectories would exhibit changing patterns and at what perturbation levels, we propose to consider a simulation ensemble with different shape parameters of the table, compute a large amount of trajectories for each ensemble member, and use visual analysis methods to explore the generated data.

To analyze the trajectories of a single ensemble member, we propose to visualize them in a phase space spanned by the positions of collisions along the boundary and directions. To analyze the changes when altering the table's parameters we compute pairwise dissimilarities between corresponding trajectories of ensemble members. These dissimilarities can be visually encoded using a multidimensional scaling (MDS) approach, which allows for the analysis of the impact of the different table parameters on the dynamics. Having identified interesting ensemble member pairs from the MDS, we support a comparative visualization of that pair by highlighting the deviations in the trajectories.

While dynamical billiards (Birkhoff, 1927) have been investigated in great depth, it has not yet been addressed in detail whether other dynamics such as symplectic billiards (Albers and Tabachnikov, 2018) exhibit similar phenomena. We apply our approach to dynamical billiards to validate our approach and to symplectric billiards for novel findings.

2 RELATED WORK

In the visualization community, there have been many attempts in trying to visually analyze dynamics. Tricoche et al. (Tricoche et al., 2012) study conservative dynamical systems using area-preserving maps. They apply their method to two example dynamics to reveal salient structure in the spatial domain. Boeing et al. (Boeing, 2016) investigated chaos and self-

Boshe-Plois, S., Ngo, Q., Albers, P. and Linsen, L.
Visual Analysis of Billiard Dynamics Simulation Ensembles.
DOI: 10.5220/0008956201850192
In *Proceedings of the 15th International Joint Conference on Computer Vision, Imaging and Computer Graphics Theory and Applications (VISIGRAPP 2020) - Volume 3: IVAPP*, pages 185-192
ISBN: 978-989-758-402-2; ISSN: 2184-4321

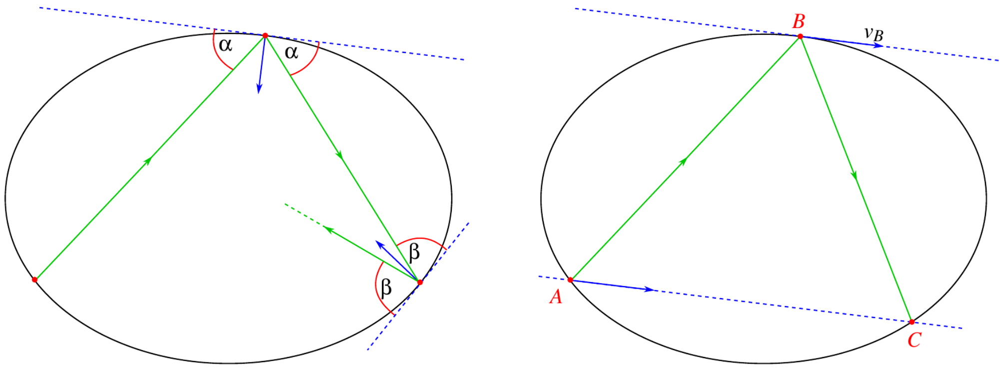

(a) standard dynamics (b) symplectic dynamics

Figure 1: Billiard dynamics.

similarity in non-linear systems. Ngo et al. (Ngo et al., 2016) investigated dynamics on networks, where they compute similarities between the dynamics of the networks' nodes, which are then visualized using a multi-dimensional scaling (MDS) approach. We also make use of MDS to visualize our data, but apply it to compare simulation runs within an ensemble of simulations. Kumpf et al. (Kumpf et al., 2019) investigated ensembles to performed a sensibility analysis for weather forecasts based on correlation measures. There aim was to identify regions of robust prediction, which is related to parts of our goals. Further approaches for dynamical systems exist in other application scenarios. To our knowledge, this is the first paper that investigates how visualization can support the analysis of billiard dynamics.

3 BACKGROUND AND REQUIREMENT ANALYSIS

We first want to provide the mathematical background for our investigations. A billiard model consists of a table and dynamics. A *billiard table* is a convex domain $\Gamma \subset \mathbb{R}^2$ with a smooth boundary $\gamma := \partial\Gamma$. Of great interests are, in particular, *elliptic billiard tables* defined via a function $F : \mathbb{R}^2 \to \mathbb{R}$ with $F(x,y) = \frac{x^r}{a} + \frac{y^w}{b} - 1$, $a,b > 0$, and $r,w \geq 2$. The elliptic billiard table's boundary is given by $\gamma = \{(x,y) \mid F(x,y) = 0\}$. Γ is called a standard elliptic table, if $r = w = 2$, otherwise a perturbed elliptic table.

The *billiard dynamics* consist of a rule set or algorithm that determines a sequence of *collision points* $(A_n)_{n\in\mathbb{N}}$ with $A_n \in \gamma$, which we call *billiard trajectory*. One may simply imagine a massless billiard ball that moves with unit speed and without friction. The most natural kind of billiard dynamics are the *dynamical* or *Birkhoff billiards*, as they arise from the laws of elastic collision in physics. Therefore, we also refer to them as *standard dynamics*. Assume we have a collision point A on the boundary γ together with a direction vector $v_A \in \mathbb{R}^2$. Then, from a point A with direction v_A, the subsequent point B is obtained as the intersection of the line $A + r \cdot v_A,\ r \in \mathbb{R}$ with γ and the subsequent direction is determined via the reflection law, i.e., the angle of incidence is the same as the angle of reflection, see Figure 1(a).

The standard dynamics can be described as a variational problem: If $A,B,C \in \gamma$ is a sequence of collisions and we fix A and C, then the position of B is defined by the condition that $|AB| + |BC|$ is extremal. In *symplectic billiards* the dynamics are derived from a related variational problem by the condition that the area of the triangle ABC is extremal (Albers and Tabachnikov, 2018). The name symplectic arises from the fact that the map describing the dynamics has the standard symplectic form ω as a generating function. Further mathematical details on the form ω are beyond the scope of this paper. It suffices to report that the resulting rules for the dynamics can be reduced to taking the position of B to be such that the vector $C - A$ lies in the tangent space $T_B\gamma$. For computing trajectories on elliptical tables, we start with two points A and B, compute the tangent $v_B \in T_B\gamma$, and calculate the root of the function $F(A + r \cdot v_B)$, see Figure 1(b) (Albers and Tabachnikov, 2018).

While structures in dynamical billiards have already been analyzed in much detail, advances for symplectic billiards are recent. Initial questions that are to be answered and respective expectations were formulated by the domain scientists as follows:

- On a standard elliptic table, one would expect clear structures that should be qualitatively independent of parameters a and b for both dynamical and symplectic billiards.

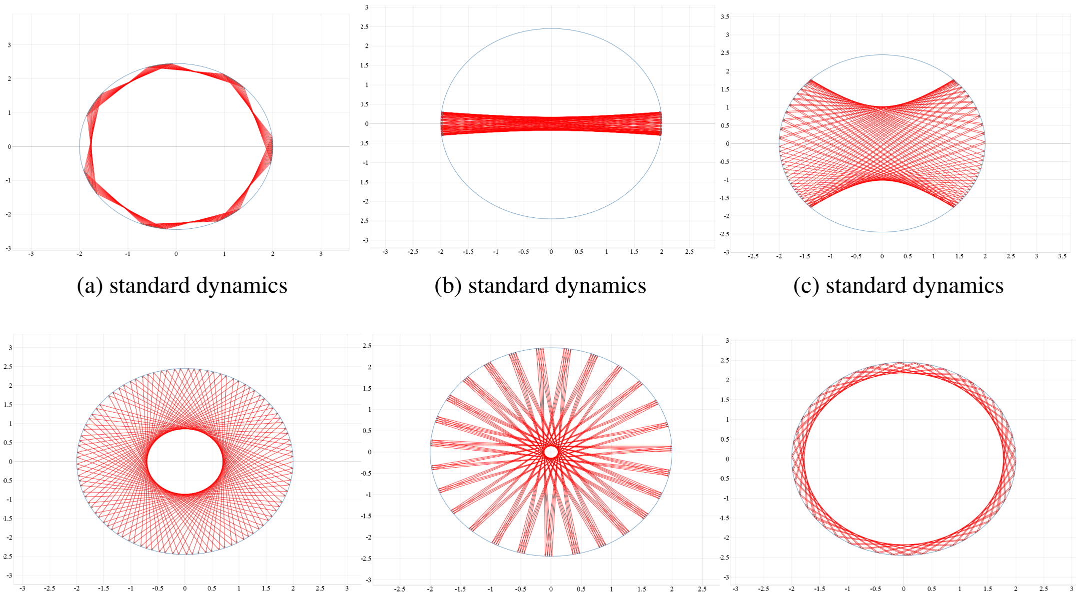

(a) standard dynamics (b) standard dynamics (c) standard dynamics

(d) symplectic dynamics (e) symplectic dynamics (f) symplectic dynamics

Figure 2: Trajectories with different starting conditions using boundary function $F(x,y) = x^2/4 + y^2/6 - 1$.

- On a perturbed elliptic table, there should occur small anomalies (i.e., trajectories change in qualitative aspects) for dynamical billiards, but it is an open question, whether the same is true for symplectic billiards.
- If some trajectories change qualitatively when perturbing the elliptic table, one would like to know how they look like.
- It is unclear what happens, if one changes the parameters a and b on a perturbed elliptic table. It would be interesting to see, whether there exist relations between the two parameters depending on their ratio.

To answer these questions, we generate and visually analyze simulation ensembles for both dynamical and symplectic billiards by varying parameters r and w as well as parameters a and b. For each ensemble member, we compute a large amount of trajectories with different starting collisions and directions for a sufficiently large number of collisions.

From the expectations and questions formulated by the domain scientists, we extracted the requirements to our analysis system as follows:

1. The highest-level goal is understand the influence of the parameter settings on the dynamics. Hence, we need to analyze the entire ensemble simultaneously.
2. When two ensemble runs differ, it would be of interest to see, which of their trajectories differ. Hence, we need a comparative visualization of trajectories of two runs.
3. On the lowest level, one is interested in observing individual simulation runs and observe the behavior of their trajectories.

4 VISUAL ANALYSIS

In this section, we describe the visualization methods we developed for analyzing individual ensemble members, ensemble member pairs, and entire ensembles.

4.1 Phase-space Visualization

Our first aim is to visualize trajectories of a single ensemble member (cf. Requirement 3). A straightforward visual encoding of a simulation outcome is to render the trajectories on the table. Figure 2 shows respective examples for standard and symplectic billiards. The visualizations clearly exhibit patterns, but only for a single trajectory. Obviously, displaying many such trajectories simultaneously leads to visual clutter. Therefore, we propose to visualize the set of trajectories for a single ensemble member in a phase-space configuration.

A phase space Ω for dynamical billiards consists of a collision point on the boundary together with a direction vector, i.e., $\Omega = \gamma \times \mathbb{R}^2$. Equivalently, it

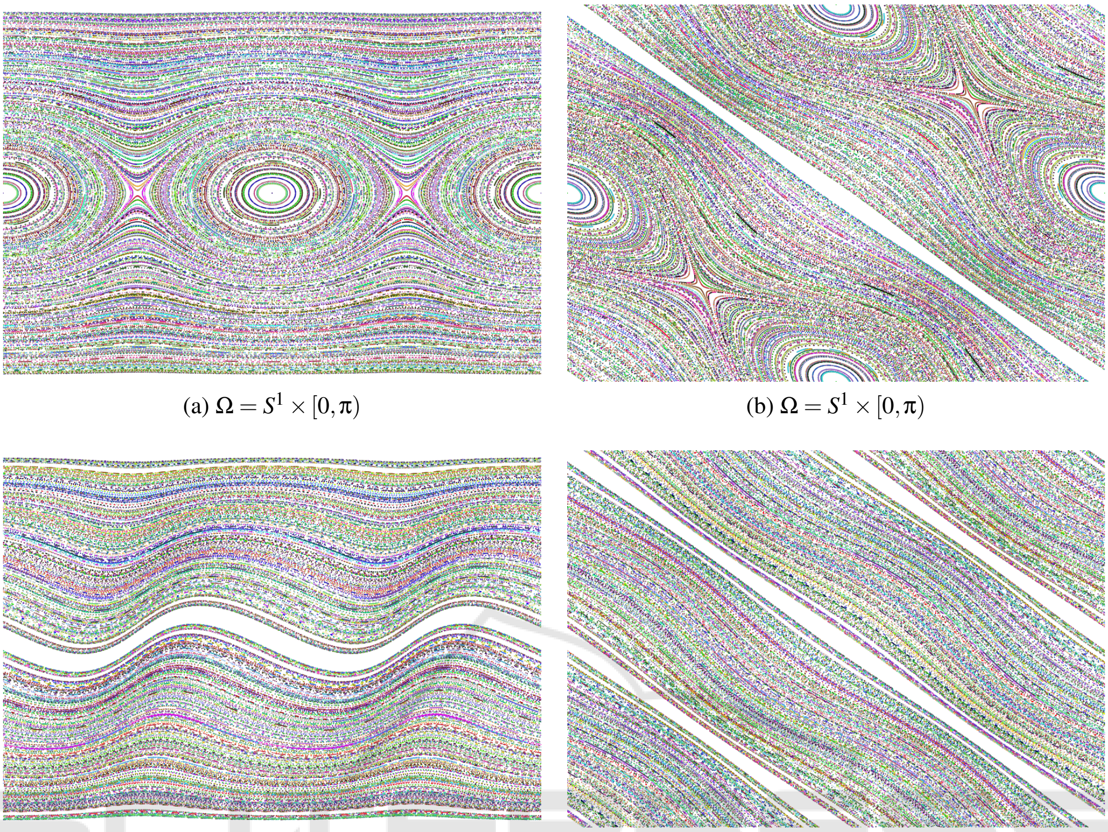

(a) $\Omega = S^1 \times [0, \pi)$ (b) $\Omega = S^1 \times [0, \pi)$

(c) $\Omega = S^1 \times S^1$ (d) $\Omega = S^1 \times S^1$

Figure 3: Phase-space visualizations of sets of trajectories (with random color mapping) using boundary function $F(x, y) = x^2/4 + y^2/6 - 1$ for standard (a,b) and symplectic dynamics (c,d).

can be defined by describing the direction using the angle to the tangent at the collision point, i.e., $\Omega = \gamma \times [0, \pi]$. Furthermore, one can apply a parametrization to the curve γ. Since γ is closed, we denote such a parametrization as $\alpha : S^1 \to \gamma$, which is equivalent to $\alpha : [s,t] \to \gamma$ with $\alpha(s) = \alpha(t)$. The phase space then becomes $\Omega = S^1 \times [0, \pi]$ or $\Omega = [s,t] \times [0, \pi]$. For elliptical tables, we chose the parametrization $\alpha(p) = \arccos(\langle p - q_c, v_c \rangle)$ with a center point $q_c \in \Gamma$ and a reference vector $v_c \in S^1$. We used $q_c = (0,0)$ and $v_c = (1,0)$. For symplectic billiards, a configuration is not defined by a collision point and a direction vector, but by two consecutive collision points. Hence, we define the phase space by $\Omega = S^1 \times S^1$ or $\Omega = [s,t] \times [s,t]$, respectively.

Having defined a phase space, a single trajectory can be visualized by plotting the respective collisions as dots in the phase space. A set of trajectories of a single ensemble member can, then, be shown by coloring each trajectory with a unique color. For the color mapping we considered categorical color maps, but given the large amount of trajectories, there are not enough colors that can be sufficiently well distinguished. Thus, random color mapping worked equally well, i.e., each trajectory just got a randomly assigned color. Figure 3 shows respective examples for standard and symplectic billiards.

4.2 Comparative Visualization

Our Requirement 2 was to visually compare two ensemble members to observe where and how trajectories differ, e.g., to highlight anomalies. From the juxtaposed phase-space visualizations in Figure 4(a,b), we can conclude that it is difficult to detect small differences. Hence, the design choice would be to compute an explicit visual encoding of computed differences. To highlight the differences, we have to compute the differences between two ensemble members. More precisely, we have to compute the differences of corresponding trajectories in the two ensemble members. Using the phase-space representation of starting configurations for trajectory computations, we can generate matching starting conditions for each ensemble member. Hence, when comparing two ensemble members, we have a set of pairs of cor-

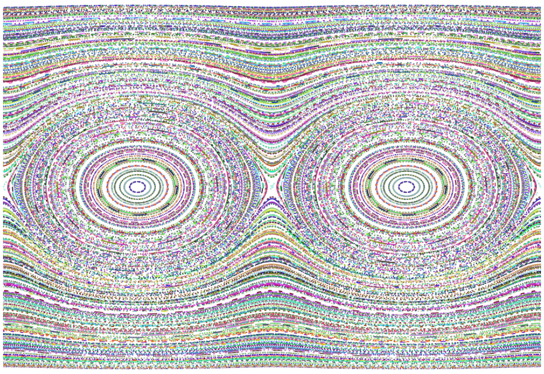

(a) standard elliptic table

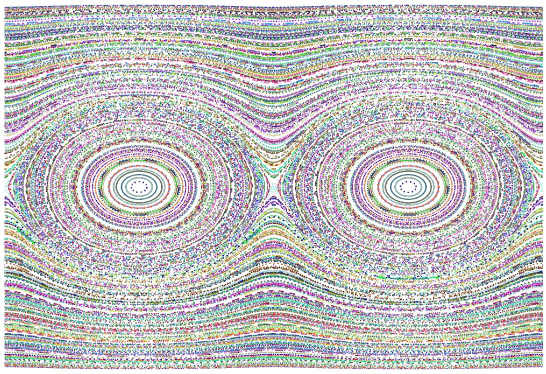

(b) perturbed elliptic table

(c) comparative visualization

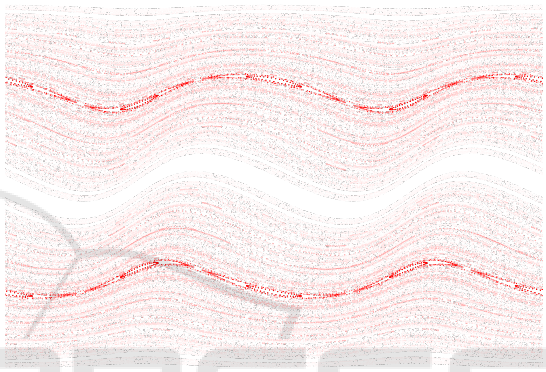

(d) symplectic dynamics

Figure 4: Juxtaposed visualization of two simulation runs using standard dynamics with parameters (a) $a = 7, b = 4, r = 2, w = 2$ and (b) $a = 7, b = 4, r = 2.001, w = 2$. (c) The comparative visualization highlights differences based on color mapping the trajectories' distances d_t. (d) When perturbing the standard elliptic table ($a = 4$, $b = 6$, $r = w = 2$) by increasing parameters $r = 2.001$ and $w = 2.005$, the comparative visualization for symplectic dynamics highlights qualitative changes in the form of cyclic structures.

responding trajectories.

Let $A = (A_j)_{1 \leq j \leq n}$ and $B = (B_j)_{1 \leq j \leq n}$ be a pair of corresponding trajectories. We define the difference of two collision points using a Euclidean metric by

$$d_c(A_j, B_j) = \left(|A_{j,1} - B_{j,1}|_T^2 + |A_{j,2} - B_{j,2}|_T^2\right)^{\frac{1}{2}}$$

with $|x-y|_T = \min(|x-y|, l - |x-y|)$ being the distance of two points in an interval quotient space with length l homeomorphic to S^1. The difference of the trajectories is, then, defined as the average difference of the collision points, i.e.,

$$d_t(A, B) = \frac{\sum_{j=1}^{n} d_c(A_j, B_j)}{n} .$$

Having computed the distances $d_t(A, B)$ for all trajectory pairs, we can highlight those trajectories A (or B respectively), where the differences are strongest. We achieve this by a applying a color mapping to the trajectories that maps the distances (after normalization to the unit interval) linearly from a background color to a foreground color. Thus, the more different trajectory A is from trajectory B the more it is emphasized. Figure 4(c) shows such a comparative visualization of two ensemble members.

4.3 Ensemble Visualization

Our final aim is to fulfill Requirement 1, i.e., to allow for an analysis of an entire ensemble to investigate the impact of the simulation parameters. Thus, we need to compare ensemble members at a global scale. Let S_1 and S_2 be two simulation runs each containing m trajectories $A^{(i)}_{1 \leq i \leq m}$ and $B^{(i)}_{1 \leq i \leq m}$. Building upon the distance metric $d_t(A^{(i)}, B^{(i)})$ for corresponding trajectory pairs, we define the difference between two simulation runs by the average of the distances of all corresponding trajectory pairs, i.e., we define

$$d_s(S_1, S_2) = \frac{\sum_{i=1}^{m} d_t(A^{(i)}, B^{(i)})}{m} .$$

We compute this distance for each pair of simulation runs in a given ensemble. The pairwise distances for

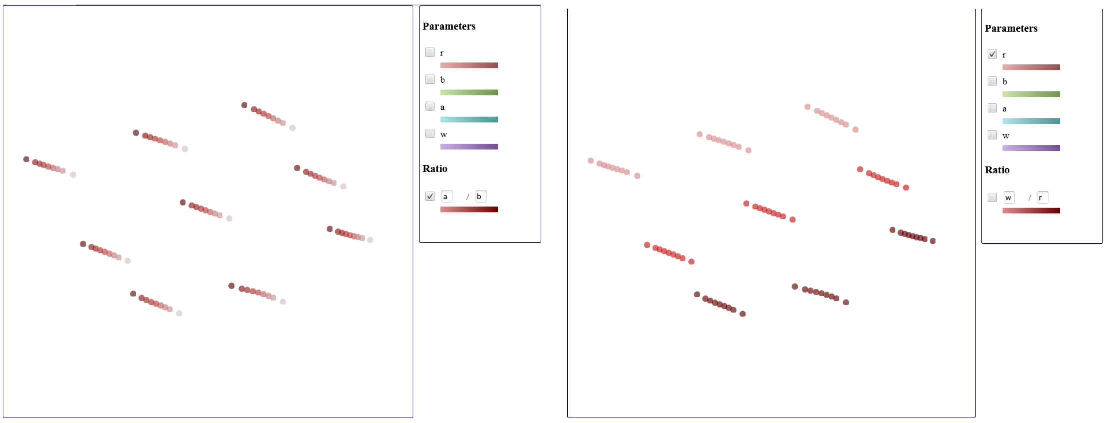

(a) influence of ratio a/b (b) influence of parameter r

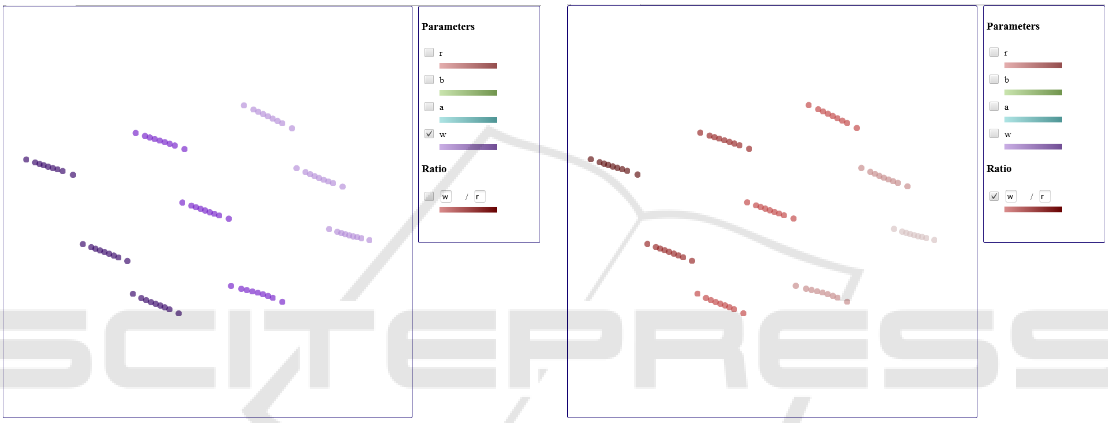

(c) influence of parameter w (d) influence of ratio r/w

Figure 5: Color coding the MDS plots by parameter values for symplectic billiards ensemble shows that r and w are the key parameters.

an ensemble of k simulation runs can be stored in a symmetric $k \times k$ distance matrix

$$D = (d_s(S_i, S_j))_{1 \leq i,j \leq k} \ .$$

The ensemble visualization shall depict the similarities (or distances) of all ensemble members. Hence, we want to find a 2D embedding, where the 2D Euclidean distances of the points that represent the ensemble members in the embedding resemble the distances stored in distance matrix D. This is exactly the objective of the classical metric multi-dimensional scaling (MDS) approach. Of course, plenty of other embeddings exist in literature, but MDS reflects our goal of preserving the computed distances by minimizing the stress function (Kruskal and Wish, 1978). For the implementation, we follow the standard solution via an eigendecomposition of the Gram matrix (Jung,).

The outcome of the MDS step is visualized in the form of a 2D scatterplot. Since our goal is to detect the influence of the billiard table's parameter, we support color mapping of the scatterplot with respect to interactively selected parameters or their ratio, see Figure 5.

5 RESULTS AND DISCUSSION

We apply our methods to simulation ensembles for standard and symplectic billiard dynamics to answer the questions raised in Section 3. We first investigated the impact of the choice of parameters a and b by considering a circular table ($a = b = 1$, $r = w = 2$) and perturbing it slightly ($a = 1.002$). For standard dynamics, the phase-space visualizations on a circular table exhibits straight trajectories, as the angles are not changing, see Figure 6(a). However, when altering parameter a slightly, the behavior changes qualitatively, as trajectories with periodic orbits emerge, see Figure 6(b). This finding confirms what was expected and known from literature. Surprisingly though, this

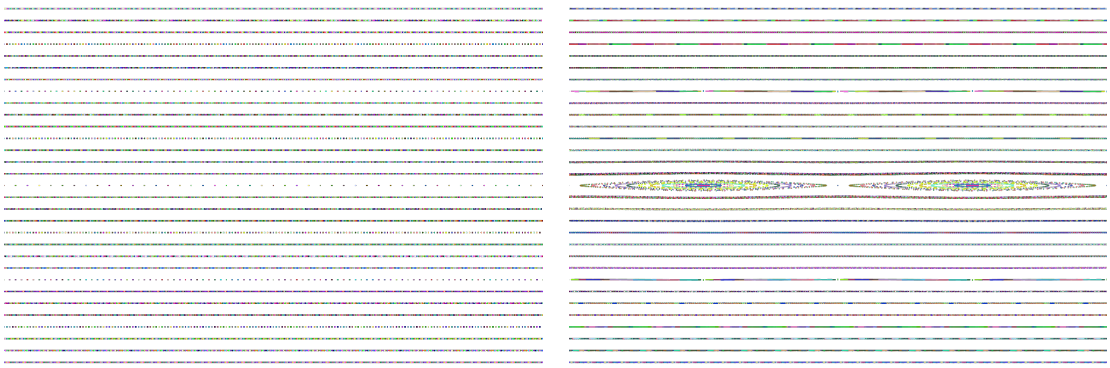

(a) $a = 1$ (b) $a = 1.002$

Figure 6: Phase-space visualizations of standard dynamics on circular (a) and slightly perturbed circular table (b) show the emergence of qualitatively different trajectories when changing parameter a.

was not true for symplectic dynamics, where phase-space visualization for the perturbed table remained qualitatively equivalent to Figure 6(a). When increasing the ellipticity of the table (e.g., further increasing parameter a), the phase-space visualizations for standard dynamics exhibit more and more orbit structures, see Figure 3(a), while phase-space visualization for symplectic dynamics still consists of horizontal curves but with waves of increasing amplitudes, see Figure 3(b).

As a second investigation, we looked into the impact of the choice of parameters r and w by comparing a standard elliptic table to a perturbed one. For standard dynamics, the phase-space visualizations seem almost identical when slightly increasing r from 2 to 2.001, see Figure 4(a,b), but the comparative visualization exhibits some structural changes, see Figure 4(c). In this investigation, the same holds true for symplectic dynamics: The comparative visualization in Figure 4(d) highlights emerging cyclic structures for perturbed tables, which have not been observed for the standard elliptic table (cf. Figure 3(b)).

Based on these initial investigation, we generated ensembles with many different parameter configurations. For standard dynamics, we generated initial collisions by sampling the phase space equidistantly with 23 position $\times$ 31 direction samples. For each initial collision, we computed a trajectory with 200 collision points. These 23×31 trajectories are computed for each ensemble member, where the ensemble is formed by choosing parameters from ranges $a \in [4; 4.004]$, $b \in [5; 5.001]$, $r = 2$, and $w \in [2; 2.009]$ with step size 0.001. The MDS plot exhibits an arc shape, see Figure 7. Color coding the plot to investigate the impact of the parameter, we can make the following observations: The color transitions for parameters a, b, or their ratio a/b confirm the observation from above that these parameters locally affect the outcome, see Figure 7(b,c). The color transitions in Figure 7(b,c) form clusters, i.e., we see groups of points where colors go from dark to bright and then this pattern is repeated for the next group. Investigating the influence of parameter w in Figure 7(a) provides a different picture: There is a trend of having brighter colors to the left of the arc and darker colors to the right, but the transition is not monotonic. However, when investigating the color transition for ratio r/w in Figure 7(d), we observe that there is a monotonic color transition from bright to dark that clearly follows the arc. Hence, we can formulate the supposition that ratio r/w is the dominant factor for significant changes, as runs occur the more similar in the MDS plot the more they have a similar ratio. This is in accordance with earlier studies in the field.

Finally, we generate a simulation ensemble for symplectic dynamics using the same initial collisions and trajectory lengths as above, while choosing parameters from ranges $a \in [4; 4.006]$, $b \in [6; 6.006]$, $r \in [2; 2.006]$, and $w \in [2; 2.006]$ with step size 0.001. Here, such studies had not been performed yet, but is easily supported by our tool. Figure 5 shows that parameters r and w and their ratio r/w are, again, responsible for generating main trends and clusters in the MDS plots, while parameters a, b and their ratio a/b are only responsible for small variations within the clusters. Figure 5(a) clearly shows the color transitions only within each of the nine clusters for the ratio a/b. For parameter r, there is a transition that creates three stripes of brightness from the upper left to the lower right. Similarly, for parameter w, there is a transition that creates three stripes of brightness from the lower left to the upper right. When combining the two parameters by looking at their ratio r/w, there is a transition from left to right with five stripes. Hence, we can conclude that for both standard and symplectic dynamics changes of ratio r/w dominate

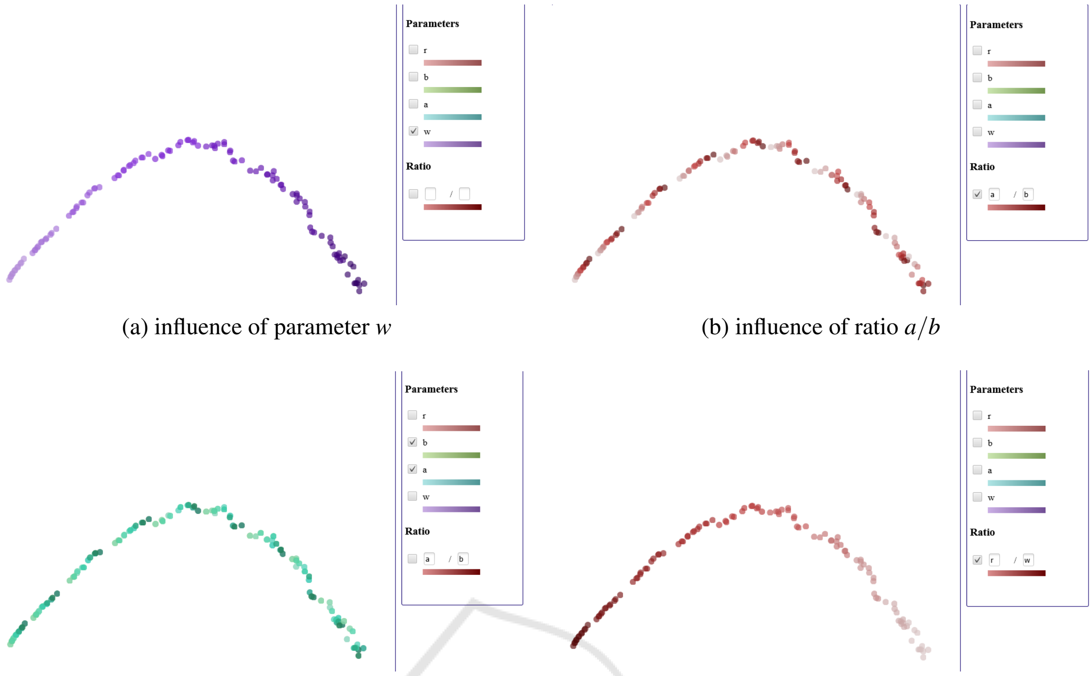

(a) influence of parameter w (b) influence of ratio a/b

(c) influence of parameters a and b (d) influence of ratio r/w

Figure 7: The main structure in the MDS visualization of the standard billiards ensemble is governed by ratio r/w.

over changes of ratio a/b. This is a novel finding that had not been reported yet.

6 CONCLUSION

We have presented a novel approach to analyze billiards using ensemble visualizations. For standard dynamics, we were able to confirm prior studies, while for symplectic dynamics we made new discoveries leading to suppositions that are a good starting point for theoretical proofs.

REFERENCES

Albers, P. and Tabachnikov, S. (2018). Introducing symplectic billiards. *Advances in Mathematics*, 333:822 – 867.

Birkhoff, G. (1927). *Dynamical Systems*. American Mathematical Society / Providence, Estados Unidos. American Mathematical Society.

Boeing, G. (2016). Visual analysis of nonlinear dynamical systems: Chaos, fractals, self-similarity and the limits of prediction. *Systems*, 4:37.

Jung, S. Lecture Notes: Multidimensional scaling, Advanced Applied Multivariate Analysis.

Kruskal, J. and Wish, M. (1978). *Multidimensional Scaling*. Number Nr. 11 in 07. SAGE Publications.

Kumpf, A., Rautenhaus, M., Riemer, M., and Westermann, R. (2019). Visual analysis of the temporal evolution of ensemble forecast sensitivities. *IEEE Transactions on Visualization and Computer Graphics*, 25(1):98–108.

Ngo, Q. Q., Hütt, M.-T., and Linsen, L. (2016). Visual Analysis of Governing Topological Structures in Excitable Network Dynamics. *Computer Graphics Forum*, 35(3):301–310.

Tabachnikov, S. (2005). *Geometry and billiards*. Student Mathematical Library. 30. American Mathematical Society, Providence, RI; Mathematics Advanced Study Semesters, University Park, PA,.

Tricoche, X., Garth, C., Sanderson, A., and Joy, K. (2012). *Visualizing Invariant Manifolds in Area-Preserving Maps*, pages 109–124. Springer Berlin Heidelberg, Berlin, Heidelberg.